Materials Science and Engineering B 178 (2013) 263–266

Contents lists available at SciVerse ScienceDirect

Materials Science and Engineering B

journal homepage: www.elsevier.com/locate/mseb

Short communication

Antireflection and band gap extension effects of ZnO nanocrystalline films grown on ITO-coated glasses by low temperature process

Xichang Bao[a,1], Yun Yang[a,b,1], Ailing Yang[b], Ning Wang[a], Ting Wang[a], Zhengkun Du[a], Chunpeng Yang[a], Shuguang Wen[a], Renqiang Yang[a,*]

[a] Qingdao Institute of Bioenergy and Bioprocess Technology, Chinese Academy of Sciences, Qingdao 266101, People's Republic of China
[b] Department of Physics, Ocean University of China, Qingdao 266100, People's Republic of China

ARTICLE INFO

Article history:
Received 5 June 2012
Received in revised form 7 November 2012
Accepted 25 November 2012
Available online 7 December 2012

Keywords:
Antireflection effect
ZnO nanocrystalline films
Band gap

ABSTRACT

Zinc oxide (ZnO) nanocrystalline films coated on indium tin oxides (ITO, 90:10 wt%) glasses were prepared by low temperature process. The thin films were composed of uniform nanoparticles with average diameter around 8.4 nm. All samples exhibited excellent optical antireflective phenomena, and the maximum transmission reached 92.8% for the sample spin coated at 1500 rpm at 453 nm, improved by 21.5%. The antireflective results were explained by the coherence theory. And the antireflective effects were induced by the ITO and ZnO films. The calculated thicknesses of the ZnO films agreed well with the experimental results. The theoretical calculated band gap from the average diameter of ZnO nanoparticles was also well consistent with the experimental ones obtained from the optical transmission spectra. This result was promising for applications in organic solar cells.

1. Introduction

Non-toxicity and low cost Zinc Oxide (ZnO) which is an ideal material in the II–VI group semiconductors with wide direct band gap energy of 3.37 eV has potential applications in many areas [1], such as optoelectronic devices [2,3], surface acoustic devices [4], sensors [5], and as electron transport layers in solar cells and light emitting diodes [6,7], etc. ZnO thin film is also one kind of high permeability and high refractive index materials, so it can be used as an antireflective candidate through reasonable designing [8]. Furthermore, ZnO nanocrystalline films may have more novel optical and electrical properties than bulk crystals owing to quantum confinement effects. So far, more unique behaviors are continuously being explored [9–12]. Further understanding the electronic and optical characterizations of ZnO nanoparticles is important for fundamental science and photonic application. For the wide variety of applications and novel properties, various methods have been used to prepare ZnO nanocrystalline films. Sputtering [13], thermal deposition [14], and chemical vapor deposition (CVD) [15] need expensive equipments, which increase the costs. Compared with these physical methods, sol–gel method is widely adopted for the fabrication of ZnO due to its simplicity, safety, no need of costly vacuum system and a cheap method for large area coating [16,17].

Nowadays, organic solar cells have emerged as one of the promising devices because they can be manufactured cost effectively by spin coating or printing on flexible substrates [6,18]. The standard architecture is fabricated on indium tin oxides (ITO) coated glass substrate as one electrode and another metal as the other electrode. In these flexible devices, ZnO closely meets the prerequisite properties of an ideal electron transport layer for wide band gap and good positioning of the conduction band of ZnO (−4.4 eV) in combination with [6,6]-phenyl-C61-butyric acid methyl ester [19]. However, this application needs preparation the ZnO films at low temperature, easy process and low cost. In addition, ITO-coated glass with high transmittance requires relatively thick ITO coating, which would increase the preparation cost. If high quality dense ZnO films were prepared on ITO-coated glasses by low temperature process and can lead to antireflective effect, which will have great advantages in the applications of such devices.

In this paper, ZnO nanocrystalline films were prepared successfully on ITO-coated glasses by a low temperature sol–gel process. All films with different thicknesses obtained from different spin-coating speeds exhibited good optical antireflective phenomena. Size-dependent absorption spectra were discussed and compared with the theoretical calculation from the effective mass model.

2. Experimental

For preparing the ZnO nanocrystalline films, zinc acetate dihydrate ($Zn(CH_3COO)_2{\cdot}2H_2O$, AR grade) and monoethanolamine (MEA, AR grade) were dissolved in 2-ethoxyethanol. The zinc

* Corresponding author. Tel.: +86 532 80662700; fax: +86 532 80662778.
E-mail address: yangrq@qibebt.ac.cn (R. Yang).
[1] These authors contributed equally to this work

0921-5107/$ – see front matter © 2012 Elsevier B.V. All rights reserved.
http://dx.doi.org/10.1016/j.mseb.2012.11.008

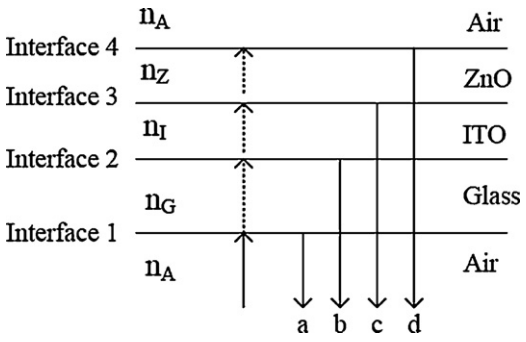

Fig. 1. Schematic diagram of the sample's structure and light path.

concentration was 0.5 mol/L. The mixture was stirred to yield a clear homogeneous solution for further use. The ITO-coated glasses were cleaned in an ultrasonic bath with acetone, ITO detergent, ultra pure water, and isopropyl alcohol for 20 min, respectively. Next, the solution was spin-coated at different speeds on the pre-cleaned ITO-coated glasses. S-X represented that the sample was spin-coated at X (X = 1000, 1500, 2000, 2500, 3000, 3500) rpm for 40 s. Subsequently, the ZnO films were dried at 100 °C in an oven for about 12 h. The schematic diagram of the sample was shown in Fig. 1, and the incident light irradiated from the side of the glass.

The surface morphologies of the ZnO nanocrystalline films were characterized by scanning electron microscopy (SEM, Hitachi 4800) and atomic force microscopy (AFM, Agilent 5400). The structure of the ZnO was studied by grazing incidence X-ray diffraction (GIXRD, Bruker D8 ADVANCE). The optical properties of the ZnO nanocrystalline films were observed by a scanning spectrophotometer (Varian Cary 50 UV/vis) in the range of 250–800 nm at room temperature. The thicknesses of ITO and ZnO nanocrystalline films were measured by Veeco Dektak150 surface profiler.

3. Results and discussion

GIXRD pattern of the ZnO nanocrystalline film was shown in Fig. 2. The grazing incidence angle is 1°. The film was prepared on a quartz glass substrate by spin coating at 1000 rpm and then treated at 100 °C in an oven for about 12 h. From Fig. 2 one can see that obvious peaks can be observed at $2\theta = 31.78°$, 34.62°, 36.08°, and 56.66°. These peaks matched well with (1 0 0), (0 0 2), (1 0 1), and (1 1 0) planes of the standard data for the wurtzite structure of ZnO (JCPDS No. 36-1451). The broad XRD peaks suggested the ZnO film was composed of nano-sized particles. According to Scherer Formula [20], the average size of nanoparticles was about 8.4 nm along the (1 0 0) peak.

Fig. 3 showed the SEM and AFM images of the ZnO nanocrystalline films prepared with different spin coating speeds. From Fig. 3(a, d and g), one can see that the ZnO film consisted of numerous homogeneous nanoparticles and the sizes of the nanoparticles were almost the same, and the sizes were independent of the spin-coating speeds. From the large scale of the SEM images (Fig. 3(b, e and h)), there was no crack formation in the films. So it was easy to prepare large homogeneous films by this method. From

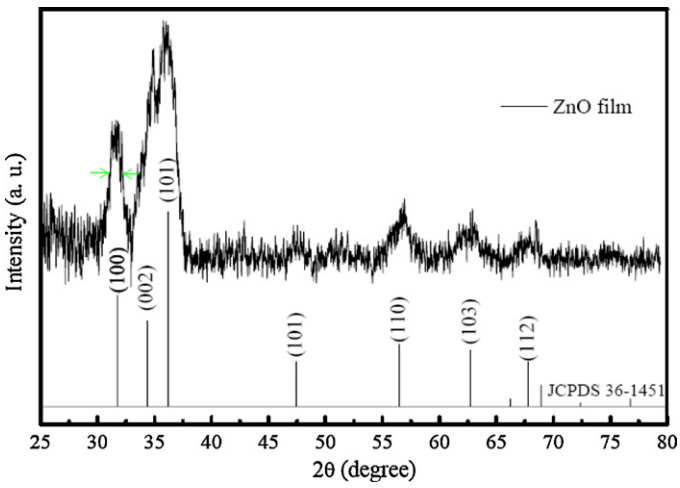

Fig. 2. GIXRD pattern of ZnO film prepared by spin coating on quartz glass at 1000 rpm (the JCPDS card of ZnO: No. 36-1451).

the AFM images of ZnO nanocrystalline films (Fig. 3 (c, f and i)), we can also see that all films were composed of uniform nanoparticles and the average size was at about 8.6 nm, which was in consistent with the calculated value by Scherer equation. The films also showed very smooth surface. In the 0.5 μm × 0.5 μm scan area, the root-mean-square roughness (RMS) of the S-1000, S-2000, and S-3000 samples were 2.27, 1.86, and 1.78 nm, respectively.

The transmission spectra of the samples with different ZnO thicknesses were shown in Fig. 4. The spectrum of the bare ITO-coated glass was included as a reference. Because of surface Fresnel reflection, the transmission of the ITO-coated glass was around 85% between 500 nm and 800 nm, and the lowest transmission was only 76.2% at 442 nm. It was interesting that all samples showed two antireflective wave bands when the ZnO thin layers were spin-coated on the bare ITO-coated glasses. The antireflection wave bands, ZnO and ITO thicknesses were summarized in Table 1. The antireflective phenomena in the wave band of 370–570 nm were more excellent than that in the wave bands of 630–800 nm. The maximum transmission improvement was relative to the thicknesses of the ZnO films. Among all samples, the transmission of sample S-1500 reached 92.8% at 453 nm, improved by 21.5%. The reflectance spectra of two samples (S-1000 and S-2500) were measured (see the insert of Fig. 4). From the insert of Fig. 4, one can see that in the visible range, the reflectance of ITO-coated glass was larger than that of the two samples, especially in the range of 370–570 nm.

Below we use the coherence theory to explain the antireflective phenomena of the samples. There are two films on the glass, ITO and ZnO. Fig. 1 shows the structure of the sample. For a vertical incident ray, it will be reflected by four interfaces. Here, ray a, b, c and d represent the reflective rays at the interfaces of air and glass, glass and ITO, ITO and ZnO, and ZnO and air. The refractive indices of air, glass, ITO and ZnO are n_A, n_G, n_I and n_Z. The thicknesses of ITO and ZnO are d_I and d_Z.

Table 1
Antireflective wave bands, and experimental thicknesses of the ZnO films and ITO film.

Sample	Wave band 1 (nm)	Wave band 2 (nm)	ZnO thickness (nm)	ITO thickness (nm)
S-3500	372–526	626–800	42 ± 2	170 ± 2
S-3000	373–530	627–800	45 ± 2	170 ± 2
S-2500	375–535	628–800	48 ± 2	170 ± 2
S-2000	380–545	630–800	52 ± 2	170 ± 2
S-1500	390–554	640–800	61 ± 2	170 ± 2
S-1000	401–570	642–800	69 ± 3	170 ± 2

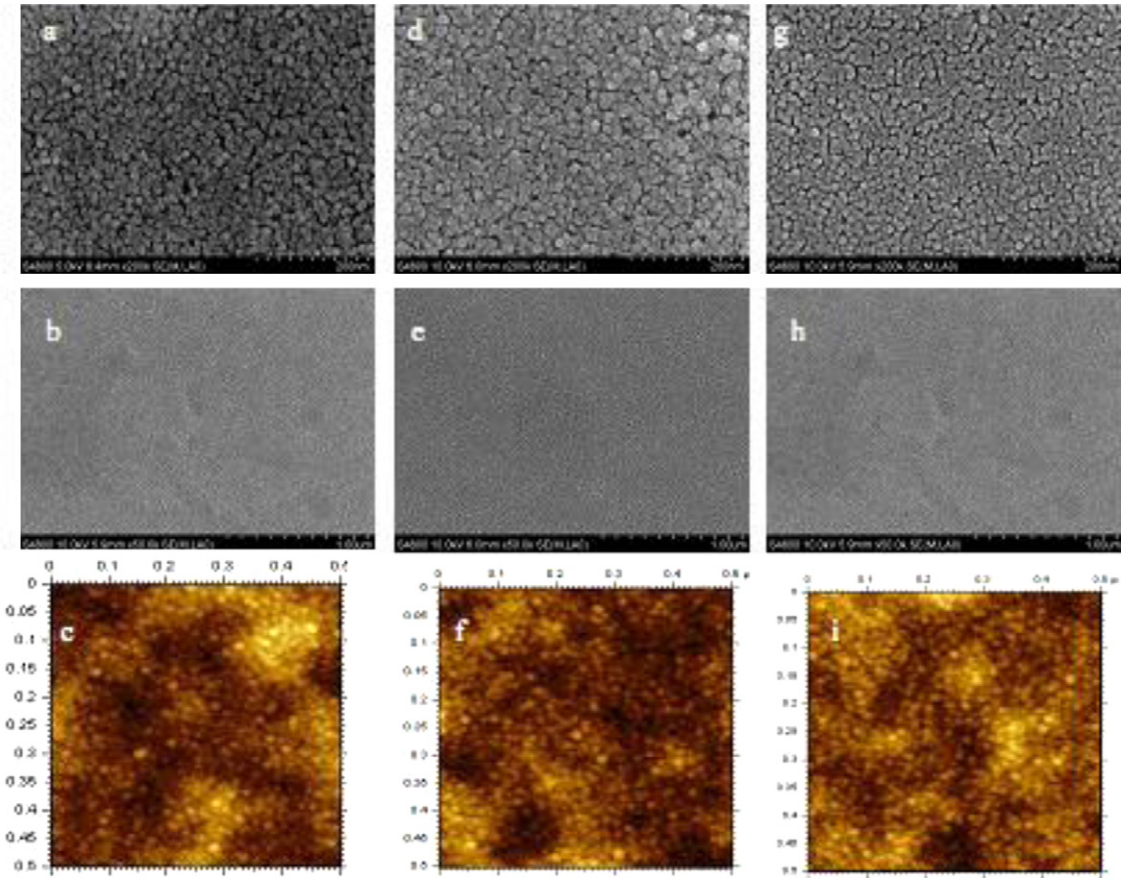

Fig. 3. SEM and AFM images of ZnO nanocrystalline films prepared with different spin coating speeds, ((a–c): S-1000, (d–f): S-2000, (g–i): S-3000).

Firstly, we consider if there is destructive coherence between ray c and d. supposing λ is the wavelength of the incident light. The optical path length difference of the two rays is $2n_Z d_z - \lambda/2$. According to the destructive coherence condition [21,22], the optical path length difference should match the following equation,

$$2n_Z d_z - \frac{\lambda}{2} = \frac{\lambda(2k+1)}{2} \quad k = 0, 1, 2 \ldots \tag{1}$$

$\lambda/2$ in Eq. (1) is for the 180° phase change occurring of ray c at the interface of ITO and ZnO. From Eq. (1), one can see the antireflective condition is relative to the refractive index and thickness of the film. For the ZnO films, according to the ref. [23,24], the refractive index of n_Z in visible range is about 2.0, so according to Eq. (1), at the maximum antireflective wavelength (453 nm), the calculated thickness of ZnO film is 103 nm for S-1500 when $k = 0$. But the experimental value is 61 nm. The calculated thickness is not consistent with our experimental data. When $k = 1, 2, 3\ldots$, the results will be further away from the experimental result. On the other hand, if we used the experimental thickness of the ZnO film, the calculated refractive index of ZnO for S-1500 is 3.67, which is far from the published results [23,24]. For the other ZnO films, one can obtain similar results. So there is no destructive coherence between ray c and ray d. For the experimental thicknesses (42–69 nm) of ZnO films, it is not reasonable to propose that the single layers of ZnO films led to the antireflection. So the antireflective effect may be induced by the ITO and ZnO films. Now we consider ray b and d, the optical path length difference between the two rays is $2n_I d_I + 2n_Z d_Z - \lambda/2$. According to the destructive coherence condition,

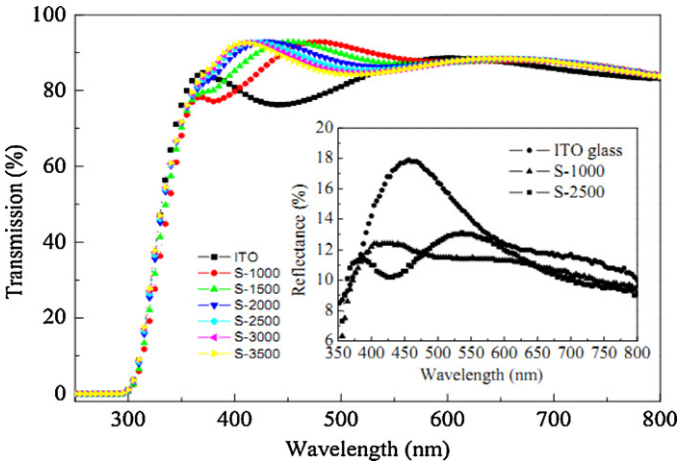

Fig. 4. Transmission spectra of the ZnO nanocrystalline films with different thicknesses controlled by spin-coating speeds, the insert is reflectance spectra.

$$2n_I d_I + 2n_Z d_Z - \frac{\lambda}{2} = \frac{\lambda(2k+1)}{2} \quad k = 0, 1, 2 \ldots \tag{2}$$

When $k = 0$, d_I is the experimental result (170 nm), n_I is 1.9 [25] and n_Z 2.0 [23], the calculated value of d_Z is equals negative values at the maximum antireflective wavelengths, which is not reasonable. But for $k = 1$, the calculated thicknesses (d_Z) of ZnO films are 77, 65, 54, 49, 46, and 43 nm for S-1000, S-1500, S-2000, S-2500, S-3000, and S-3500, respectively. The theoretical results are well consistent with the experimental data. Therefore, the antireflective effect is induced by the ITO and ZnO films.

From Fig. 4, one can see that the absorption edges had a slight red shift when ZnO films were coated on ITO-coated glasses. For a direct band gap semiconductor, the corresponding optical band

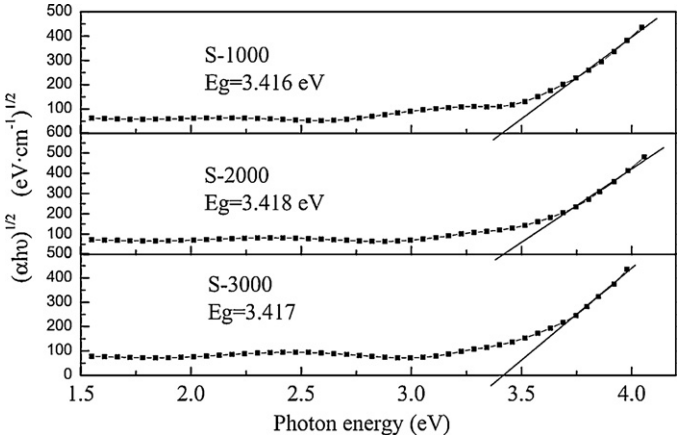

Fig. 5. Three representative band gaps of ZnO nanocrystalline films.

gaps of these films can be estimated by extrapolation of the linear relationship between $(\alpha h\upsilon)^{1/2}$ and $h\upsilon$. According to Tauc-Sounds equation [26],

$$\alpha h\upsilon = B(h\upsilon - E_g)^2 \tag{3}$$

where α is the absorption coefficient per unit length, which is determined from its transmission (T), i.e.,

$$\alpha = \frac{\ln T}{d} \tag{4}$$

where d is the thickness of the thin film, h Planck's constant, and hυ the incident photon energy. According to Eqs. (3), (4) and Fig. 4, the optical band gaps are 3.414 eV, 3.417 eV, 3.412 eV, 3.418 eV, 3.413 and 3.416 eV for S-3500, S-3000, S-2500, S-2000, S1500, and S-1000, respectively. Three representative results (S-1000, S-2000 and S-3000) are shown in Fig. 5. The calculated band gaps are almost the same. These results show that the ZnO nanocrystalline films prepared with different spin coated speeds are composed of homogeneous nanoparticles with same sizes, and the sizes of the nanoparticles are independent of the spin speeds. Comparing with the bulk ZnO materials, the band gaps of the ZnO films have an extension of ~0.045 eV, which may be due to the quantum size effect of ZnO nanoparticles [27].

We can also analyze the band gap extension of the ZnO films on the ITO-coated glasses. It is well known that there is a relationship between band gap and size of nano-spherical particle [27–29]. Assuming the ZnO nanoparticle is a sphere, and considering the effective-mass model for a spherical particle with a Coulomb interaction term, the band gap of ZnO can be estimated by the following approximate equation [24],

$$E_g \cong E_g^{bulk} + \frac{h^2}{2eD^2}\left(\frac{1}{m_e} + \frac{1}{m_h}\right) - \frac{1.8e}{2\pi\varepsilon_0\varepsilon_r D} \tag{5}$$

where E_g^{bulk} is the energy gap of bulk material, e the charge of electron, D the diameter of nanoparticle, ε_0 and ε_r the vacuum and relative dielectric constants, m_e and m_h the effective masses of electron and hole, respectively. We chose $E_g^{bulk} = 3.37$ eV, $m_e \cong 0.26\, m_0$, $m_h \cong 0.59\, m_0$, $\varepsilon_r = 8.5$ [29] and $D = 8.4$ nm, According to applied Eq. (5), the calculated band gap is 3.415 eV, which is well consistent with the band gap energy obtained from the optical transmission spectra.

4. Conclusion

In summary, the ZnO nanocrystalline films were successfully prepared by the low-temperature process and characterized by SEM, AFM, and XRD. The thin films were composed of uniform nanoparticles with average diameter around 8.4 nm. All samples exhibited excellent optical antireflective phenomena, and the maximum transmission reached 92.8% for S-1500 at 453 nm, improved by 21.5%. The antireflective results were explained by the coherence theory. Theoretical analysis showed that the single layers of ZnO films with thicknesses of 42–69 nm on the ITO-coated glasses can't cause antireflective phenomena. And the antireflective effects were induced by the ITO and ZnO films. The calculated thicknesses of the ZnO films agreed well with the experimental results. The band gaps (E_g) calculated by the effective-mass model for spherical particles with a Coulomb interaction term were well consistent with the experimental ones obtained from optical transmission spectra. The results of this work are promising for improving the performance of inverted organic solar cells with ZnO nanocrystalline films as electron transport layers.

Acknowledgements

This work was supported by National Natural Science Foundation of China (61107090, 51173199), Ministry of Science and Technology of China (2010DFA52310), CAS ("One Hundred Talented Program", and KGCX2-YW-399+9-2), Department of Science and Technology of Shandong Province (2010GGC10345), and Qingdao Municipal Science and Technology Program (11-2-4-22-hz).

References

[1] S.J. Pearton, D.P. Norton, K. Ip, Y.W. Heo, T. Steiner, Progress in Materials Science 50 (2005) 293.
[2] J.B. Baxter, E.S. Aydil, Applied Physics Letters 86 (2005) 053114.
[3] S. Chu, G. Wang, W. Zhou, Y. Lin, L. Chernyak, J. Zhao, J. Kong, L. Li, J. Ren, J. Liu, Nature Nanotechnology 6 (2011) 506.
[4] V. Chivukula, D. Ciplys, M. Shur, P. Dutta, Applied Physics Letters 96 (2010) 233512.
[5] Q. Wan, Q.H. Li, Y.J. Chen, T.H. Wang, X.L. He, J.P. Li, C.L. Lin, Applied Physics Letters 84 (2004) 3654.
[6] Y. Sun, J.H. Seo, C.J. Takacs, J. Seifter, A.J. Heeger, Advanced Materials 23 (2011) 1679.
[7] J.S. Park, B.R. Lee, E. Jeong, H.J. Lee, J.M. Lee, J.S. Kim, J.Y. Kim, H.Y. Woo, S.O. Kim, M.H. Song, Applied Physics Letters 99 (2011) 163305.
[8] Y.J. Lee, D.S. Ruby, D.W. Peters, B.B. McKenzie, J.W.P. Hsu, Nano Letters 8 (2008) 1501.
[9] H.M. Cheng, K.F. Lin, H.C. Hsu, W.F. Hsieh, Applied Physics Letters 88 (2006) 261909.
[10] M.K. Patra, M. Manoth, V.K. Singh, G.S. Gowd, V.S. Choudhry, S.R. Vadera, N. Kumar, Journal of Luminescence 129 (2009) 320.
[11] X.Q. Zhang, S.L. Hou, H.B. Mao, J.Q. Wang, Z.Q. Zhu, Applied Surface Science 256 (2010) 3862.
[12] H. Wei, M. Li, Z. Ye, Z. Yang, Y. Zhang, Materials Letters 65 (2011) 427.
[13] W.M. Li, H.Y. Hao, Journal of Materials Science 47 (2012) 3516.
[14] W.Z. Xu, Z.Z. Ye, Y.J. Zeng, L.P. Zhu, B.H. Zhao, L. Jiang, J.G. Lu, H.P. He, S.B. Zhang, Applied Physics Letters 88 (2006) 173506.
[15] J.P. Biethana, V.P. Sirkeli, L. Considinea, D.D. Nedeoglob, D. Pavlidisa, H.L. Hartnagel, Materials Science and Engineering B 177 (2012) 594.
[16] E.J. Luna-Arredondo, A. Maldonado, R. Asomoza, D.R. Acosta, M.A. Melendez-Lira, M.L. lvera, Thin Solid Films 490 (2005) 132.
[17] N.R.S. Farley, C.R. Staddon, L.X. Zhao, K.W. Edmunds, B.L. Gallagher, D.H. Gregory, Journal of Materials Chemistry 14 (2004) 1087.
[18] H. Oh, J. Krantz, I. Litzov, T. Stubhan, L. Pinna, C.J. Brabec, Solar Energy Materials and Solar Cells 95 (2011) 2194.
[19] A.L. Linsebigler, G. Lu, J.T. Yates Jr., Chemical Reviews 95 (1995) 735.
[20] Z.G. Ji, S.C. Zhao, C. Wang, K. Liu, Materials Science and Engineering B 117 (2005) 63.
[21] Germain Chartier, Introduction to Optics (Springer, New York,2005), p 259-298.
[22] B.G. Prevo, Y. Hwang, O.D. Velev, Chemistry of Materials 17 (2005) 3642.
[23] C. Besleaga, G.E. Stan, A.C. Galca, L. Iona, S. Antohe, Applied Surface Science 258 (2012) 8819.
[24] B. Huang, J. Li, Y.B. Wu, D.H. Guo, S.T. Wu, Materials Letters 62 (2008) 1316.
[25] Y.S. Jung, Solid State Communications 129 (2004) 491.
[26] Q.X. Zhang, W.S. Wei, F.P. Fang, Chinese Physics B 20 (2011) 047802.
[27] K.F. Lin, H.M. Cheng, H.C. Hsu, L.J. Lin, W.F. Hsieh, Chemical Physics Letters 409 (2005) 208.
[28] L.E. Brus, Journal of Chemical Physics 80 (1984) 4403.
[29] E.M. Wong, P.G. Hoertz, C.J. Liang, B.M. Shi, G.J. Meyer, P.C. Searson, Langmuir 17 (2001) 8362.